

Title	Direct imaging of atomic clusters in an amorphous matrix: A Co-C granular thin film
Author(s)	Sato, Kazuhisa; Mizuguchi, Masaki; Tang, Ruihe et al.
Citation	Applied Physics Letters. 2012, 101(19), p. 191902
Version Type	VoR
URL	<a href="https://hdl.handle.net/11094/89405">https://hdl.handle.net/11094/89405</a>
rights	This article may be downloaded for personal use only. Any other use requires prior permission of the author and AIP Publishing. This article appeared in Kazuhisa Sato, Masaki Mizuguchi, Ruihe Tang, Jung-Goo Kang, Manabu Ishimaru, Koki Takanashi, and Toyohiko J. Konno, "Direct imaging of atomic clusters in an amorphous matrix: A Co-C granular thin film", Appl. Phys. Lett. 101, 191902 (2012) and may be found at <a href="https://doi.org/10.1063/1.4765362">https://doi.org/10.1063/1.4765362</a> .
Note	

***Osaka University Knowledge Archive : OUKA***

<https://ir.library.osaka-u.ac.jp/>

Osaka University

## Direct imaging of atomic clusters in an amorphous matrix: A Co-C granular thin film

Kazuhisa Sato, Masaki Mizuguchi, Ruihe Tang, Jung-Goo Kang, Manabu Ishimaru et al.

Citation: *Appl. Phys. Lett.* **101**, 191902 (2012); doi: 10.1063/1.4765362

View online: <http://dx.doi.org/10.1063/1.4765362>

View Table of Contents: <http://apl.aip.org/resource/1/APPLAB/v101/i19>

Published by the [American Institute of Physics](#).

---

### Related Articles

Germanium nano-cluster films as humidity and hydrogen sensors

*J. Appl. Phys.* **112**, 074514 (2012)

Probing into hybrid organic-molecule and InAs quantum-dots nanosystem with multistacked dots-in-a-well units

*J. Appl. Phys.* **112**, 064903 (2012)

Determination of ion track radii in amorphous matrices via formation of nano-clusters by ion-beam irradiation

*Appl. Phys. Lett.* **101**, 103112 (2012)

Three-dimensional fabrication and characterisation of core-shell nano-columns using electron beam patterning of Ge-doped SiO<sub>2</sub>

*Appl. Phys. Lett.* **100**, 263113 (2012)

Perpendicular magnetization in CoO (111) layers induced by exchange interaction with ferromagnetic Co and Ni<sub>60</sub>Cu<sub>40</sub> nanoclusters

*J. Appl. Phys.* **111**, 083901 (2012)

---

### Additional information on *Appl. Phys. Lett.*

Journal Homepage: <http://apl.aip.org/>

Journal Information: [http://apl.aip.org/about/about\\_the\\_journal](http://apl.aip.org/about/about_the_journal)

Top downloads: [http://apl.aip.org/features/most\\_downloaded](http://apl.aip.org/features/most_downloaded)

Information for Authors: <http://apl.aip.org/authors>

## ADVERTISEMENT



**Goodfellow**  
metals • ceramics • polymers • composites  
70,000 products  
450 different materials  
**small quantities fast**

[www.goodfellowusa.com](http://www.goodfellowusa.com)

## Direct imaging of atomic clusters in an amorphous matrix: A Co-C granular thin film

Kazuhiro Sato,<sup>1,a)</sup> Masaki Mizuguchi,<sup>1</sup> Ruihe Tang,<sup>1</sup> Jung-Goo Kang,<sup>1</sup> Manabu Ishimaru,<sup>2</sup> Koki Takanashi,<sup>1</sup> and Toyohiko J. Konno<sup>1</sup>

<sup>1</sup>*Institute for Materials Research, Tohoku University, Sendai 980-8577, Japan*

<sup>2</sup>*Institute of Scientific and Industrial Research, Osaka University, Ibaraki 567-0047, Japan*

(Received 26 September 2012; accepted 17 October 2012; published online 6 November 2012)

The atomic structure of extremely small cobalt (Co) nanoparticles embedded in an amorphous carbon (C) matrix has been studied by spherical aberration ( $C_s$ ) corrected high-resolution transmission electron microscopy and focal-series restoration. The Co nanoparticles, 1–3 nm in diameter, are crystalline with the face centered cubic structure, while the radial distribution function analysis revealed the existence of a Co–C bond. The reconstructed phase images of the exit-wave function clearly show the projected potential distribution within the Co nanoparticles. The  $C_s$ -correction has hence a benefit to visualize embedded crystalline clusters unambiguously, which are responsible for the magnetotransport properties of the Co-C films. © 2012 American Institute of Physics. [<http://dx.doi.org/10.1063/1.4765362>]

Granular magnetic thin films, consisting of ferromagnetic metal nanoparticles embedded in a non-magnetic medium, have been actively studied in the last two decades due to their novel magnetic and magnetotransport properties.<sup>1–4</sup> Among several granular systems, Co nanoparticles dispersed in an amorphous carbon (a-C) matrix are one of the well-known systems intensively investigated in the past.<sup>5–9</sup> In general, granular films can be characterized by particle size, shape, packing density, and crystal structure of the granules. From a practical point of view, an interesting feature that makes the Co-C system quite unique is the fact that the electric conductivity of the a-C matrix can be tuned as well by controlling these structural parameters. Until now, some studies focused on the magnetic properties of Co-C films,<sup>5–9</sup> yet, their magnetotransport mechanism has not been elucidated so far. Recently, some of the authors have reported a large negative magnetoresistance (MR) of 27.6% at 2 K under 90 kOe for co-sputtered Co-C granular thin films.<sup>10</sup> Although this study demonstrated novel temperature-dependent magnetotransport phenomena in Co-dilute Co-C granular thin films, their atomic structure still remains an open question.

In this study, aberration ( $C_s$ ) corrected transmission electron microscopy (TEM) was used for atomic level observation to determine the structure of embedded Co nanoparticles 1–3 nm in diameter in the aforementioned Co-C granular film. In addition to highly improved spatial resolution,  $C_s$ -corrected TEM has a benefit of smaller defocus values under optimal defocus conditions, which is suitable for imaging extremely small atomic clusters with less contrast delocalization at particle surfaces and/or internal defects.

Co-C granular thin films were deposited onto Si(100) substrates by a magnetron co-sputtering technique.<sup>10</sup> High purity Co (>99.9%) and C (>99.999%) targets were used as source materials. The base pressure was lower than  $2 \times 10^{-5}$  Pa, and the deposition was carried out in an argon (Ar) atmosphere (0.21 Pa) at room temperature. We fabricated Co-C thin films with a thickness of 90 nm after 4 h of deposition. The

Co content was determined to be 6.4 at. % by elemental analysis using an electron probe micro-analyzer.<sup>10</sup> Cross-sectional TEM samples were prepared by a tripod polishing technique in combination with Ar ion milling. Two types of TEMs, both operating at 300 kV with a field emission gun, were used. For atomic structure imaging, we used an FEI Titan 80–300 TEM equipped with a  $C_s$ -corrector for the objective lens together with detectors for a bright-field (BF) and a high-angle annular dark-field (HAADF) scanning TEM (STEM). All high-resolution TEM (HRTEM) images were recorded using a charge coupled device (CCD) camera attached to the TEM. Electron diffraction patterns were obtained using a JEOL JEM-3000F TEM with imaging plates (Fuji Film, FDL-UR-V) for radial distribution function analysis. Focal-series HRTEM images were reconstructed using the IWR software package (HREM Research Inc.).<sup>11</sup>

Figure 1(a) is a cross-sectional BF-STEM image of the Co-C granular thin film, showing densely distributed nanometer-sized particles with dark contrasts throughout the 90-nm-thick Co-C layer. On the other hand, in the HAADF-STEM image shown in Fig. 1(b), Co nanoparticles are imaged as bright contrasts due to atomic number ( $Z$ ) contrast. In addition, Fig. 1(c) shows result of elemental analysis by energy dispersive x-ray spectroscopy (EDS), taken with a spread beam, where small peaks from the Co compared to that of C suggest that the average Co content of the film is low.

Figure 2(a) shows a HRTEM image and the corresponding selected area electron diffraction (SAED) pattern of the Co-C layer. A few nanometer-sized crystalline clusters, where lattice fringes are clearly seen, are distributed in an a-C matrix, while the SAED pattern shows only halo rings arising from a-C. The lattice fringes shown here indicate that these Co particles, 1–3 nm in diameter, possess the face centered cubic (fcc) structure with a random orientation. The presence of the fcc-Co, instead of the equilibrium hexagonal closed-packed (hcp) phase, is due to the small size, as reported for nanoparticles.<sup>12</sup> Possible structural change due to electron irradiation can be excluded in the HRTEM observation using a CCD camera with a short acquisition time of

<sup>a)</sup>Electronic mail: ksato@imr.tohoku.ac.jp.

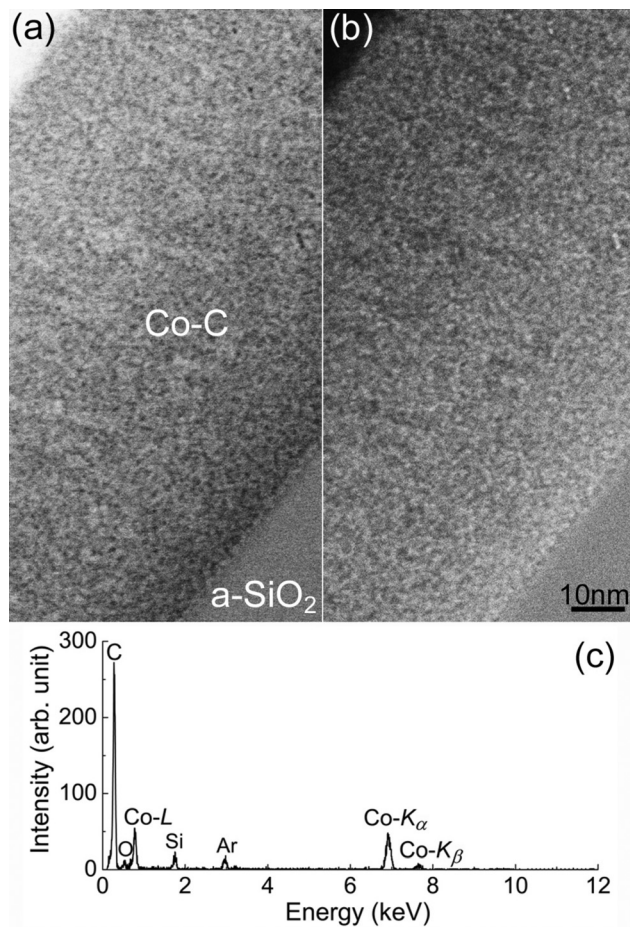


FIG. 1. A pair of (a) BF-STEM and (b) HAADF-STEM images of a cross section of the Co-C granular thin film. For the HAADF-STEM imaging, a beam convergence of 10 mrad and a detector angle greater than 60 mrad were used. (c) EDS profile measured from the Co-C layer.

1 s. However, it should be noted that prolonged irradiation, 1–2 min or longer, induced gradual coalescence and growth of Co particles. Figures 2(b) and 2(c) show typical examples of high magnification images of [100]- and [110]-oriented Co particles, respectively. The  $C_s$  was adjusted to 8.7  $\mu\text{m}$  and thus the theoretical optimal defocus (Scherzer focus) becomes as small as 4.8 nm, which is approximately 10 times smaller than that required for a conventional TEM with a  $C_s$  value of 1 mm or so. As a result, the atomic structure of clusters can be clearly imaged at a defocus value close to the just focus condition. In Fig. 2(b), {002} lattice fringes of the fcc structure are seen in the 1 nm-sized particle, whereas {111} lattice fringes and a faceted particle shape are seen in the 2 nm-sized particle shown in Fig. 2(c). In these images atomic positions appear as dark contrasts, which are in good agreement with those calculated. Figure 2(d) shows a histogram of the particle size, which is well-fitted with a log-normal type distribution function with the average size of 1.9 nm, corresponding to approximately 500 constituent atoms. Thus modern  $C_s$ -corrected HRTEM unambiguously revealed the formation of crystalline Co nanoparticles 1–3 nm in diameter, while the formation of amorphous Co grains was concluded in the literature.<sup>7</sup> Note that imaging such small clusters using conventional HRTEM is quite sensitive to astigmatism, defocus, and sample thickness.

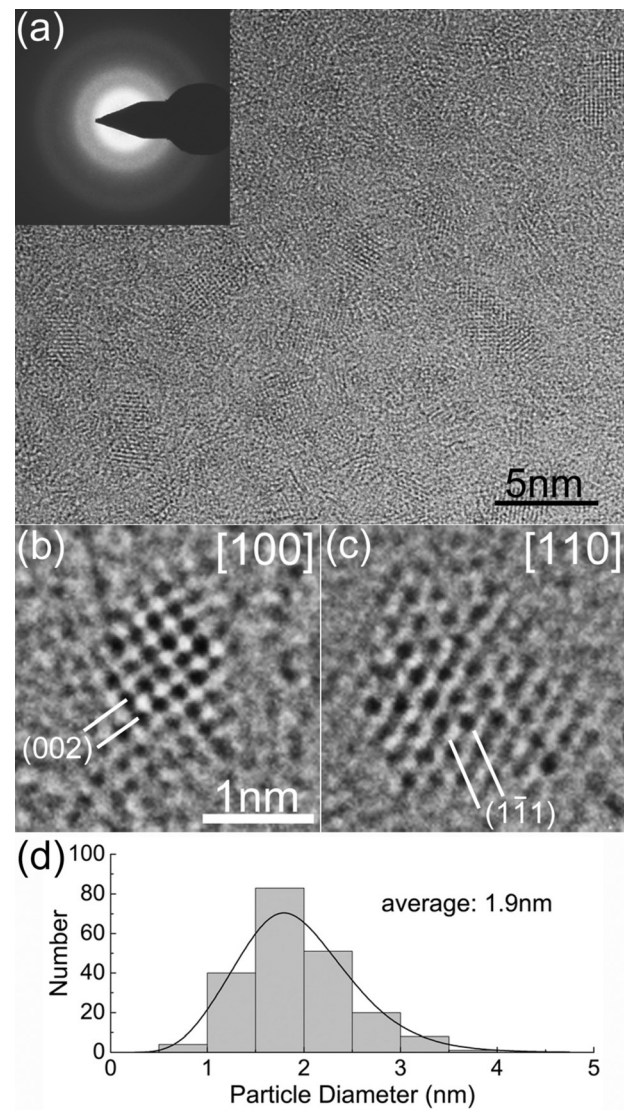


FIG. 2. (a)  $C_s$ -corrected HRTEM image and the corresponding SAED pattern of the cross section of a Co-C granular thin film. (b) High magnification images of 1 nm-sized [100]-oriented fcc-Co cluster and (c) 2 nm-sized [110]-oriented one. (d) Histogram of particle size distribution of Co granules. The average size is 1.9 nm with  $\ln \sigma$  of 0.27.

Figure 3 shows phase images of the exit-wave function obtained after reconstructing a focal series of HRTEM images taken at  $C_s = 8.7 \mu\text{m}$ . In the reconstruction process, we used five successive images with the defocus step of 2 nm, and a reconstructed phase image, in principle, excludes any effect of lens aberration or defocusing. Figure 3(a) shows the phase image of a [110]-oriented fcc-Co cluster. In

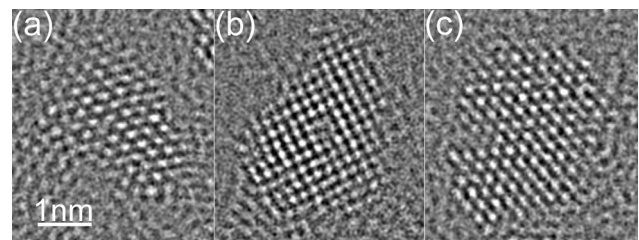


FIG. 3. Phase images of fcc-Co clusters obtained by focal-series restoration. Particle sizes are (a) 2 nm, (b) 2.7 nm, and (c) 2.9 nm. Surface atom arrangements are clearly seen.

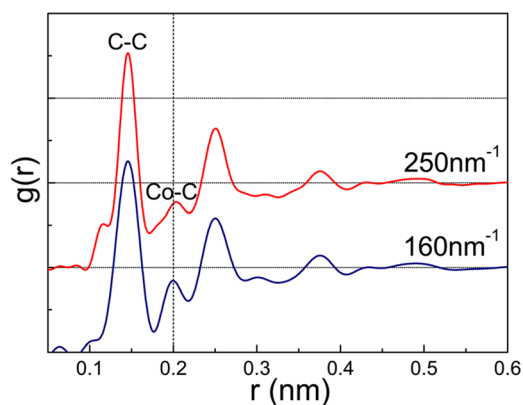


FIG. 4. The experimentally measured pair distribution function  $g(r)$  of the co-sputtered Co-C granular thin film. These profiles were obtained by different scattering vectors. A weak subpeak at  $0.204 \pm 0.004$  nm suggests the presence of the Co-C bond.

this case, the reconstruction converged after four cycles of iteration. Periodic arrangement of atoms is clearly seen as bright contrast. Note that within the framework of weak phase object approximation, the contrast in the phase image corresponds directly to the projected electrostatic potential distribution within the specimen. However, it has been reported that the phase shift is sensitive to surface atomic configuration of nanoparticles,<sup>13</sup> and therefore, a quantitative analysis of the phase is not straightforward. Figures 3(b) and 3(c) are other examples of the phase images of [100]-oriented and [110]-oriented fcc-Co clusters, respectively. As a result of focal-series restoration, overall, atomic arrangement of the faceted particle interface is unambiguously imaged with a less contrast of amorphous carbon matrix.

To further confirm the atomic structure of the Co-C film, we examined radial distribution functions by a quantitative analysis of electron diffraction intensities.<sup>14,15</sup> We obtained electron diffraction patterns from the entire Co-C layer at 100 K using a cooling stage to reduce background intensities as well as to avoid contamination. Intensity profiles with weak signals can be recorded up to scattering angles as high as  $Q \sim 250 \text{ nm}^{-1}$ . (The scattering vector is defined as  $Q = 4\pi \sin\theta/\lambda$ , where  $\theta$  and  $\lambda$  are the scattering half angle and the electron wavelength, respectively.) Figure 4 shows experimentally measured atomic pair distribution functions,  $g(r)$ , of the Co-C granular thin film. The first and second prominent peaks are centered at 0.146 and 0.250 nm, which can be assigned to the C-C bonds.<sup>16–18</sup> In addition to these peaks, a weak subpeak appears at  $0.204 \pm 0.004$  nm, which is comparable with the reported value for a Co-C bond length of  $0.194 \pm 0.002$  nm<sup>19</sup> and can be assigned to a Co-C bond in the present film. The location of this subpeak is not affected by the truncation of the scattering vector in the reciprocal lattice space, and therefore it is a real peak. The existence of the Co-C bonding can be attributed to the granular film structure with a low Co content: Co nanoparticles are surrounded by

the a-C matrix. On the other hand, the Co-Co bond length is reported to be 0.25 nm according to the literatures,<sup>19,20</sup> which entirely overlaps with that of the second nearest neighbor distance of amorphous carbon, and therefore, invisible.

In summary, we have studied atomic structure of the co-sputtered Co-C granular thin film with a large negative magnetoresistance by using HAADF-STEM,  $C_s$ -corrected HRTEM, and radial distribution function analysis. Densely packed fine Co particles in the amorphous carbon matrix were clearly visualized by Z-contrast STEM images. The Co nanoparticles are fcc single crystals with an average particle size as small as 1.9 nm. Surface atom arrangements are clearly imaged by means of focal-series phase restoration. The observed Co-C bonding can be attributed to the granular film structure with a low overall Co content.

The authors wish to thank Dr. T. Kiguchi for his support on exit-wave reconstruction and Dr. A. Hirata for valuable comments on amorphous structures. K.S. and T.J.K. appreciate supports by the Grant-in-Aid for the Challenging Exploratory Research (Grant No. 23651094) from the Ministry of Education, Culture, Sports, Science, and Technology, Japan.

- <sup>1</sup>A. E. Berkowitz, J. R. Mitchell, M. J. Carey, A. P. Young, S. Zhang, F. E. Spada, F. T. Parker, A. Hutten, and G. Thomas, *Phys. Rev. Lett.* **68**, 3745 (1992).
- <sup>2</sup>J. Q. Xiao, J. S. Jiang, and C. L. Chien, *Phys. Rev. Lett.* **68**, 3749 (1992).
- <sup>3</sup>A. Gerber, A. Milner, B. Groisman, M. Karpovsky, A. Gladkikh, and A. Sulpice, *Phys. Rev. B* **55**, 6446 (1997).
- <sup>4</sup>K. Yakushiji, S. Mitani, F. Ernult, K. Takanashi, and H. Fujimori, *Phys. Rep.* **451**, 1 (2007).
- <sup>5</sup>T. Hayashi, S. Hirono, M. Tomita, and S. Umemura, *Nature* **381**, 772 (1996).
- <sup>6</sup>T. J. Konno, K. Shoji, K. Sumiyama, and K. Suzuki, *J. Magn. Magn. Mater.* **195**, 9 (1999).
- <sup>7</sup>W. B. Mi, L. Guo, E. Y. Jiang, Z. Q. Li, P. Wu, and H. L. Bai, *J. Phys. D: Appl. Phys.* **36**, 2393 (2003).
- <sup>8</sup>H. Weinforth, C. Somsen, B. Rellinghaus, A. Carl, E. F. Wassermann, and D. Weller, *IEEE Trans. Magn.* **34**, 1132 (1998).
- <sup>9</sup>X. Nie, J. C. Jiang, L. D. Tung, L. Spinu, and E. I. Meletis, *Thin Solid Films* **415**, 211 (2002).
- <sup>10</sup>R. Tang, M. Mizuguchi, H. Wang, R. Yu, and K. Takanashi, *IEEE Trans. Magn.* **46**, 2144 (2010).
- <sup>11</sup>L. J. Allen, W. McBride, N. L. O'Leary, and M. P. Oxley, *Ultramicroscopy* **100**, 91 (2004).
- <sup>12</sup>O. Kitakami, H. Sato, Y. Shimada, F. Sato, and M. Tanaka, *Phys. Rev. B* **56**, 13849 (1997).
- <sup>13</sup>L. C. Gontard, L.-Y. Chang, A. I. Kirkland, C. J. D. Hetherington, D. Ozkaya, and R. E. Dunin-Borkowski, *Angew. Chem.* **46**, 3683 (2007).
- <sup>14</sup>Y. Hirotsu, M. Ishimaru, T. Ohkubo, T. Hanada, and M. Sugiyama, *J. Electron Microsc.* **50**, 435 (2001).
- <sup>15</sup>T. Takagi, T. Ohkubo, Y. Hirotsu, B. S. Murty, K. Hono, and D. Shindo, *Appl. Phys. Lett.* **79**, 485 (2001).
- <sup>16</sup>G. Galli, R. M. Martin, R. Car, and M. Parrinello, *Phys. Rev. Lett.* **62**, 555 (1989).
- <sup>17</sup>F. Finocchi, G. Galli, M. Parrinello, and C. M. Bertoni, *Phys. Rev. Lett.* **68**, 3044 (1992).
- <sup>18</sup>O. Gereben and L. Pusztani, *Phys. Rev. B* **50**, 14136 (1994).
- <sup>19</sup>D. S. Yang, I. Kim, Y. G. Yoo, and S. C. Yu, *J. Phys. Soc. Jpn.* **71**, 487 (2002).
- <sup>20</sup>B. Mierzwa, *J. Alloys Compd.* **362**, 178 (2004).